*IOSR Journal of Applied Geology and Geophysics (IOSR-JAGG)*
*e-ISSN: 2321–0990, p-ISSN: 2321–0982.Volume 8, Issue 1 Ser. II (Jan – Feb 2020), PP 11-22*
*www.iosrjournals.org*

# Artificial Neural Network Application for Optimum Prediction of Porosity in Heterogeneous Reservoir using Well logs

Sola Oluwaseun Ayantola* and John Olurotimi Amigun
*Department of Applied Geophysics, Federal University of Technology, Akure, Nigeria.*

***ABSTRACT:*** *In mitigating the challenge in oil and gas industries caused by inaccurate estimation of reservoir porosity from well log measurement due to heterogeneity nature of reservoir rocks, Artificial Neural Network (ANN) was employed for the accurate prediction of reservoir porosity. The understanding that the volume of oil, gas, and water in a reservoir depends directly on its porosity underscore the importance of having accurate porosity prediction. In this study, well logs (sonic, resistivity and density) which are known to affect the porosity within the reservoir of interest were selected as input variables of the supervised network while core porosity data of Well 1 was set as its target and trained using Levernberg-Marquadt algorithm of ANN at epoch 10. The input data were randomly divided into 75% of training, 15% of validation and 15% of testing while the mean squared error and validation regression obtained after the training were 0.000268816 and 0.999996 respectively. The produced artificial intelligence script was run to predict porosity (true porosity) of wells 2, 3, 4 and 5. Average predicted porosity of well 2 within the reservoir 'Res' 2 was 0.249 while that of well 4 was 0.326. At validation, a very good match between the ANN predicted and core porosities was obtained. The regression coefficient of the predicted against core porosities of well 2 is 0.9381 and the average percentage deviation for well 2 and 4 are 2% and 11% respectively. Excellent matching of core data and predicted values reflects the accuracy of the technique which suggests that the ANN predicted porosity model represent the true porosity distribution of reservoir (RES 2). The result of this study has been able to show the cost effectiveness without compromising the accuracy of the reservoir porosity estimation.*

***KEY WORDS:*** *Heterogeneity, Algorithm, Predicted porosity, Cost effectiveness, Accuracy*

---

Date of Submission: 13-01-2020 Date of acceptance: 29-01-2020

---

## I. Introduction

Porosity, which is one of the most important parameters for reservoir characterization, is the percentage of voids to the total volume of rock. The amount of internal space or voids in a given volume of rock is a measure of the amount of fluids a rock will hold and the volume of oil, gas, and water in a given reservoir depends directly on porosity[1]. In porosity estimation, reports indicated that a porosity of one percent is equivalent to the presence of 77.6 barrels of pore space in a total volume of one acre-foot of sand[2]. High-precision estimation of porosity is one of the challenging tasks for the oil industries due to its inherent heterogeneity and its non-linear relationship with the amount of fluid contained in a reservoir. Distinct geological ages, depositional environments and different characteristics of rocks have been given as causes of this heterogeneity[3].

Since accurate determination of reservoir porosity in the petroleum industry especially in reserve estimation at the stage of reservoir development is of great importance, core analysis being the oldest and still practiced technique usually provides accurate and precise measurement however it is highly costly, time and labour-intensive. In spite of the cost implication, only a few out of all wells are usually cored due to this cost implication. In contrast, well log data which often contain invaluable information though cheaper provide a continuous record over the entire hole are always used indirectly to estimate the reservoir properties[4]. The log measurements of reservoir porosity could be done by neutron porosity, formation density, nuclear magnetic resonance (NMR) and sonic[5] but none of the logs actually measures porosity directly. Several researchers have attempted to estimate reservoir porosities from these suites of logs (most especially electrical and sonic logs) by employing conventional method of petrophysical estimation but failed to accurately conform to the actual porosity.

From density logs, porosity has been estimated using (equation 1)[6]

$$\phi_d = \frac{\rho_{ma} - \rho_b}{\rho_{ma} - \rho_f} \quad (1)$$

where $\phi_d$= density-derived porosity; $\rho_{ma}$ = matrix density; $\rho_b$= bulk density; and $\rho_f$= fluid density.

From sonic log, porosity has also been estimated using (equation 2)[7]

$$\phi_s = \frac{\Delta_t - \Delta_{tma}}{\Delta_{tf} - \Delta_{tma}} \quad (2)$$

where $\phi_s$ = sonic-derived porosity, $\Delta_t$= transit time, $\Delta_{tf}$= fluid transit time and $\Delta_{tma}$= transit time for the rock matrix.

From equations (1 and 2), several extensions were proposed. It was further argued that natural phenomena such as porosity cannot be adequately estimated by linear relations. Since the conventional method failed to accurately estimate this reservoir property, therefore a lower cost method, which is economical and at the same time provide similar accuracy as that of core data is needed. Hence, computer-based intelligence method such as Artificial Neural Networks (ANN) provide the way out to easily handle these nonlinearity problems in an efficient manner [8,9,10,11,12]. ANN is able to provide more reliable variables of reservoir properties. This method is also independent of the inherent uncertainties present in the borehole[11].

In this study, ANN was applied to predict the reliable porosity values from the well log data taken from the 'OSA' field by setting the core porosity data as the actual porosity.

**Neural network**

Human brain is a very complex, non-linear and parallel computer system, which is capable of thinking, remembering and problem solving[13]. It has the capability to organize its structural constituents known as neurons so as to perform certain computations e.g. pattern recognition, perception etc. much faster than a computer[13]. A biological neuron is a fundamental unit of the brain's nervous system (Figure 1a). Similarly, a neural network is described as a massively parallel-distributed processor made up of simple processing units called neurons, which has a natural tendency for storing experiential knowledge and making it available for use[13]. An artificial neuron is a fundamental unit to the operation of the neural network. The block diagram of (Figure 1b) shows the model of a neuron. Its basic elements as shown in the diagram are:

(i) a set of synapses or connecting links, each of which is characterised by a weight of its own. A signal $x_j$ at the input of synapse *j* connected to neuron *k* is multiplied by the synaptic weight $w_{kj}$.

(ii) an adder for summing the input signals, weighted by the respective synapses of the neuron.

(iii) an activation function for limiting the amplitude of the output of a neuron. It limits the permissible amplitude range of the output signal to some finite value.

These elements listed above make neural network resemble the human brain in the following respects:

(i) knowledge is acquired by the network from its environment through a learning process.

(ii) interneuron connection strengths, known as synaptic weights, are used to store the acquired knowledge.

Mathematically the function of the neuron (*k*) [14] can be expressed by

$$y_k = \varphi(u_k + b_k) \quad 3$$

Where

$$u_k = \sum_{j=1}^{m} w_{kj} x_j \quad 4$$

$x_j$ is the input signal from an *m* dimensional input, $w_{kj}$ is the synaptic weights of neuron *k*, $u_k$

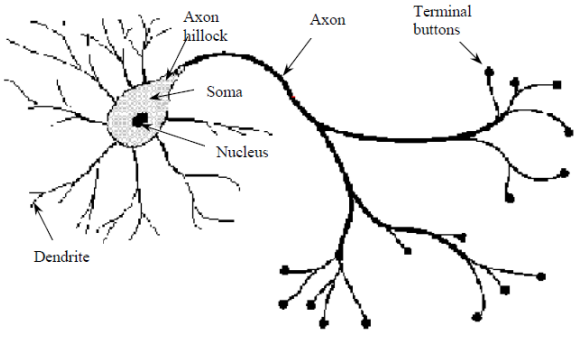


Figure 1a: Schematic of a Biological Neuron[13].

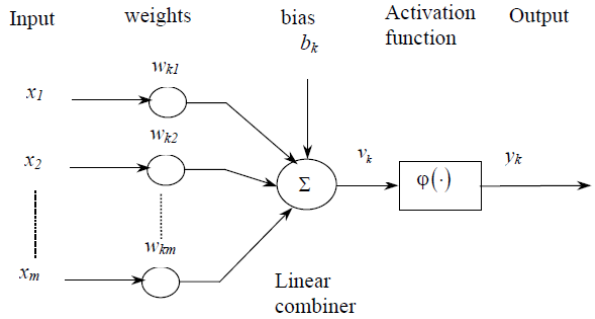


Figure 1b: Model of a Neuron showing some Basic Elements[13].

is the linear combiner output due to the input signals, $b_k$ is the bias, $\varphi$(v) is the activation function, and $y_k$ is the output signal of the neuron. The relation between the linear combiner output $u_k$ and the activation potential is $v_k$ as expressed in (equation 5)[13].

$$v_k = u_k + b_k \quad 5$$

The activation function $\varphi(v)$ defines the output of a neuron in terms of the induced local field *v*. The activation functions used is sigmoid function.

This is the most common form of activation function used in the construction of multilayer networks that are trained using back-propagation algorithm because it has the feature of being non-decreasing and differentiable and its range is $0 \leq \varphi(v) \leq 1$. An example of the sigmoid function is stated in equation 6

$$\varphi(v) = \frac{1}{1+\exp(-av)} \qquad 6$$

Whereais the slope parameter of the sigmoid function. The slope at the origin equals *a*/4. In the limit as the slope parameter approaches infinity the sigmoid function becomes a threshold function. A sigmoid function has a continuous range of values from 0 to 1. Sometimes it is desirable to have the activation function range from -1 to +1 in which case the activation function assumes an antisymmetric form with respect to the origin. Then $\varphi(v)$ can be given by hyperbolic tangent function defined by equation 7.

$$\varphi(v) = \tanh(v) \qquad 7$$

**Geology of study area**

"OSA" field is located within offshore Niger Delta, Nigeria. The base map for the survey area is shown in Figure 2. The Niger Delta is situated in the Gulf of Guinea and extends throughout the Niger Delta province[15]. It is located in the southern part of Nigeria between the longitude $5^0$E and $9^0$E and latitude $3^0$N and $6^0$N (Figure 2 and 3). It was formed at the site of a rift junction related to the opening of the south Atlantic starting in the late Jurassic and continuing into the Cretaceous[16]. Niger Delta is divided into three formations namely Benin, Agbada and Akata Formations, which is representing prograding depositional facies that are distinguished mostly on the basis of sand-shale ratios (Figure 4).

The Benin Formation is the uppermost unit, it consists of massive freshwater bearing continental sands and gravel deposited in an upper deltaic plain environment and extends from the west across the whole Niger Delta area and southward beyond the existing coastline. The thickness of the formation ranges from 305m in the offshore to 3050m onshore. The Agbada Formation which is the next formation forms the hydrocarbon-prospective sequence in the Niger Delta**.** It is composed of sands, silts and shale in various proportions and thicknesses, representing cyclic sequences of off-lap units. It reaches a maximum thickness of more than 3050 m. The Akata Formation composed of shale and silts at the base of the known delta sequence. They contain a few streaks of sand, possibly of turbiditic origin and were deposited in holomarine environment. The thickness of this sequence is not accurately known; but may reach 7000 m in the central part of the delta thickness[17].The Niger Delta province is made up of the Tertiary Niger Delta (Agbada - Akata) petroleum system (Figure 4). The primary source rock is the upper Akata Formation, the marine-shale facies of the delta with possibly contribution from interbedded marine shale of the lowermost Agbada Formation[18]. Oil is produced from sandstone facies within the Agbada Formation,

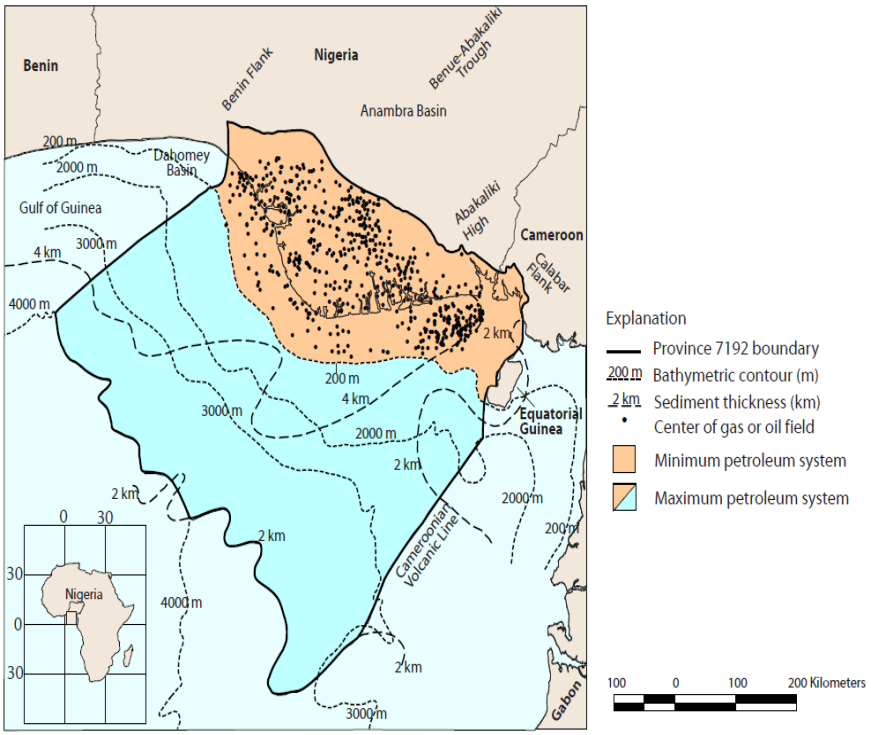


**Figure 2:** Map of Niger Delta showing Province outline (maximum petroleum system) and key structural features16.

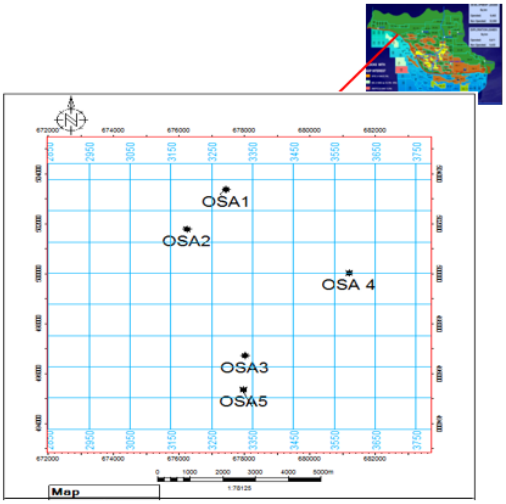


**Figure 3:** Location Map and the Base Map of the Study Area

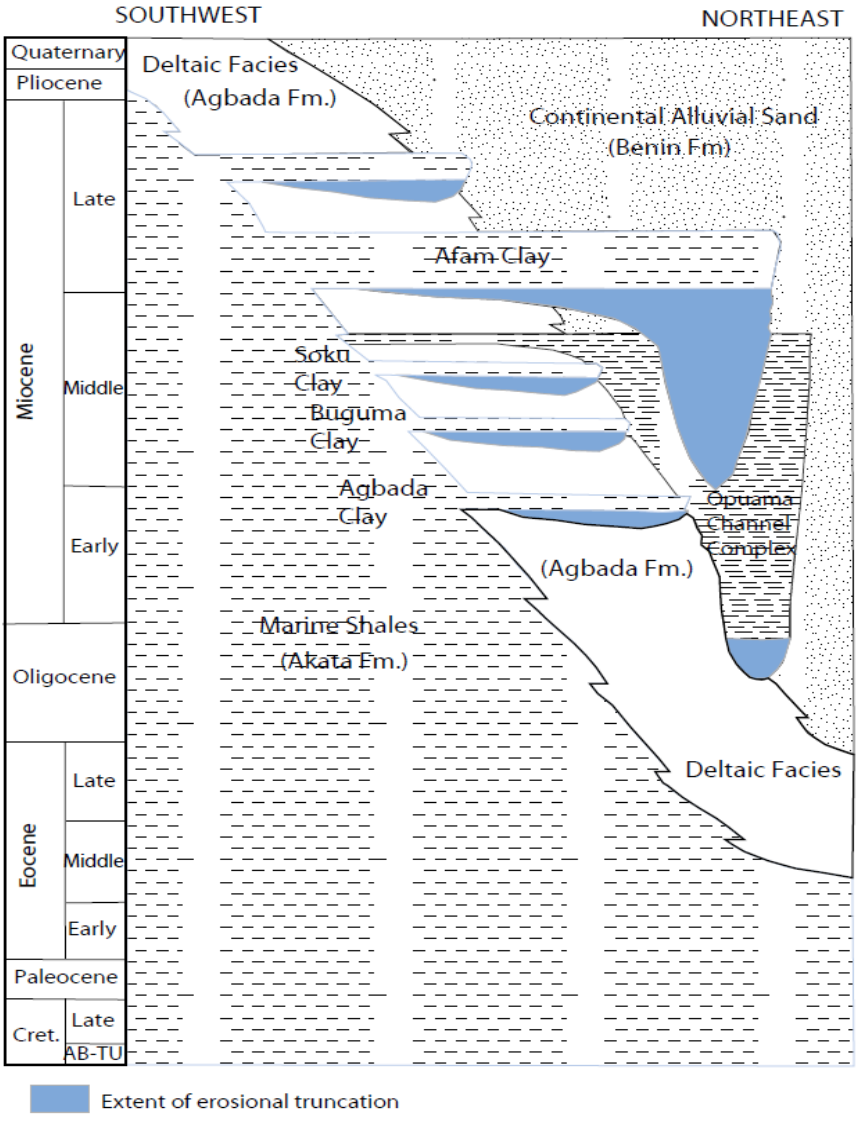


**Figure 4:** Stratigraphic column showing the three formations of the Niger Delta17,19.

however, turbidite sand in the upper Akata Formation is a potential target in deep water offshore and possibly beneath currently producing intervals onshore.
From the Eocene to the present, the delta has prograded southwestward, forming depobelts that represent the most active portion of the delta at each stage of azazzits development.

## II. Materials And Methodology

The materials used includes 3D Seismic data (Seg-Y), Suite of well logs, Checkshot survey data, Well deviation data, Core data, Software (Petrel 2014 version, Excel and MATLAB 2015 version)

**Lithostratigrahic correlation**

This was done by delineating the sand body and reservoir unit with the aid of gamma log and resistivity log respectively.
Gamma ray log was used to delineate the lithology (sand and shale units) on the basis that the gamma ray response is less in sand compared to shale. The sand line depicts minimum gamma ray response while the shale baseline was the maximum gamma ray response. The log was set to a scale of 0-150 API, central cut off of 75 API units was used in which values less than 75 API connotes sand while those greater than 75 API was interpreted to be shale.
Reservoirs are subsurface formations that contain oil and gas in commercial quantities. They were identified by using gamma ray and deep resistivity in which the zones are considered to be hydrocarbon-bearing zone while those with low resistivity were interpreted as water bearing zones.
Porosity estimate from density logs using conventional method
Having delineated the reservoir unit, porosity was estimated from density logs using equation 1(From 6)

**Porosity prediction using ANN**

Supervised learning of neural network was used in this work. The neural net is composed of three layers which are input, hidden and output layers (Figure 5). Input-output variables identification was first done before setting up the network. Three data sets (sonic, density and resistivity logs) were selected as input variables for ANN for training, validating and testing the network (Figure 6). The input data set are known to affect the porosity[20]. The Levenberg-Marquardt algorithm was adopted. The training takes less time but required more memory. This involves a forward propagation step followed by a backward propagation step. The network training started with five (5) numbers of hidden neurons followed by ten (10) neurons and finally with fifteen (15 neurons), The input variables and target variables were randomly divided into three subsets namely; (i) training, (ii) validation and (iii) test sets in ratio 5:1:1 respectively.

401 data sets comprising density, resistivity and sonic logs within the reservoir 1 unit were imported into MATLAB following the 5:1:1 ratio i.e. training equal 281; validation, 60 and test, 60.

The first subset is the training set which was used for computing the gradient and updating the network weights and biases. In accordance with the 5:1:1 ratio, the training is equivalent to 70% of the variables. The second subset is the validation set and it is 15% of the vectors and was used to measure the network generalization. The third subset is the test set which is 15% of the vectors and it role was to compare different models.
The root-mean-square error (RMSE) in (Equation 8)[21] was used to indicate the network performance. The RMSE is usually used as a measure of the global error, which is defined as:

$$\mathrm{RMSE} = \sqrt{\frac{\sum_{p=1}^{np}\sum_{k=1}^{n3}(t_{kp}-y_{kp})^2}{np.n3}} \qquad 8$$

Where:
np is the number of training patterns
n3 is the number of output neurons in the output layer (i.e. the third layer in the three-layer neural net)
t and y are the target and calculated output values respectively on these error values. At the end of the training phase, the results of plot performance and regression were presented as profiles.

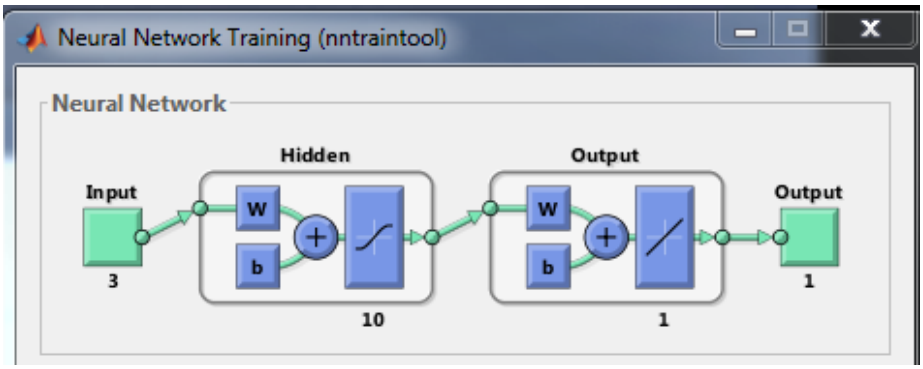


Figure 5: A Neural Network View

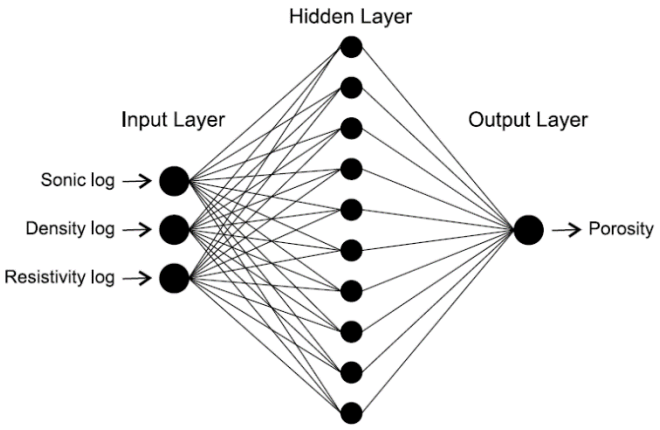


Figure 6: Architecture of the Neural Network that Predicts Porosity of the Study Area

Having trained the network perfectly, other outputs of the reservoir porosity were then generated using the neural network code of the MATLAB matrix-only function. Two of the output results were validated with their respective core data.

**Validation and statistical analysis**

Validation: This was done by correlating the predicted porosity with core porosity data in order to show the level of correlation between the predicted porosities and the true porosity (core porosity).

Statistical analysis: This was done by finding the regression and percentage deviation error was calculated to determine the level of correlation between the predicted porosities and the actual porosity (core porosity).

Percentage deviation error = $\left[\frac{\text{Actual value(X)} - \text{Predicted value(Y)}}{\text{Actual value(X)}}\right] \times 100\%$

## III. Results And Discussion

**Lithostratigraphic Correlation**

A picture of the subsurface stratification is necessary when evaluating the hydrocarbon potentials of a field to know the lateral continuity of a reservoir and faulting. The four wells that were correlated along the North West – South East direction reveals the intercalations of sand and shale unit where two reservoirs namely Res 1 and 2 were delineated (Figure 7). The field correlation indicates that the reservoirs mapped are laterally continuous and thins out southward Reservoir 'Res' 1 and 'Res' 2 falls within the depth range of 7870ft - 10040ft and 8080 - 10320ft respectively.

Reservoir 'Res' 2 of 'OSA' field which is of interest based on its hydrocarbon potential and the available corresponding core data was worked on

**NEURAL NETWORK**

Performance and regression plots of the network outputs with respect to targets for training, validation and test sets are displayed to help in evaluating the errors associated with the network in order to find the best fit of network (Figure 8). The performance was measured in terms of mean squared error and is shown in a log scale as a plot of mean square error against the epoch. The magnitude of the error changes as the network is being trained. Figure 8a shows the training at neuron 10, the best validation performance of 0.00031256 was observed at epoch 58. Another retraining of the same neuron 10 is shown in Figure 8b with best validation performance of 0.00028854 observed at epoch 260. The summary of the Validation performance and other results at different network architecture neuron 10 and 15 were presented in Table 1. Neuron 10 was thereby chosen for this study due to its better performance rating.

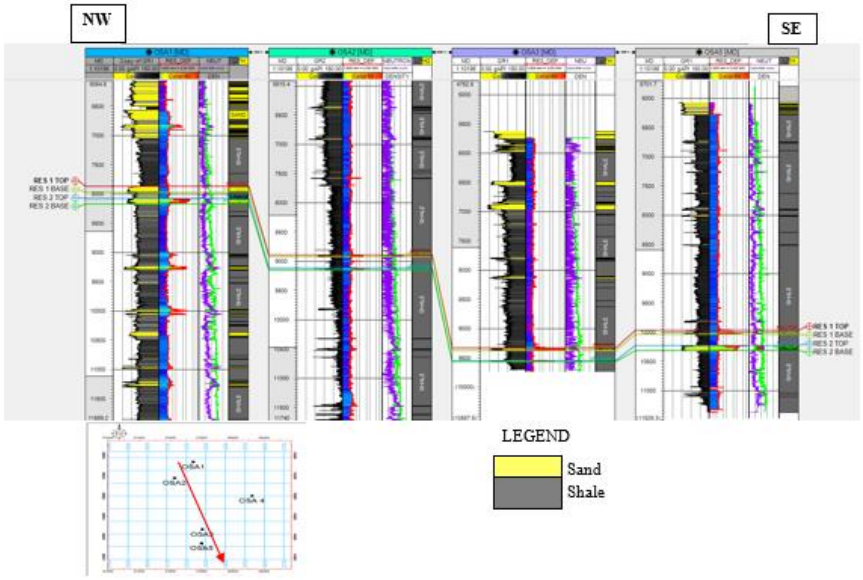


Figure 7: Correlation Pannel across Four Wells

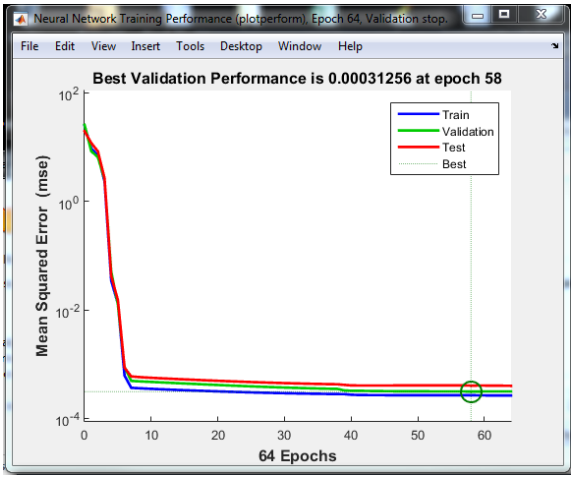


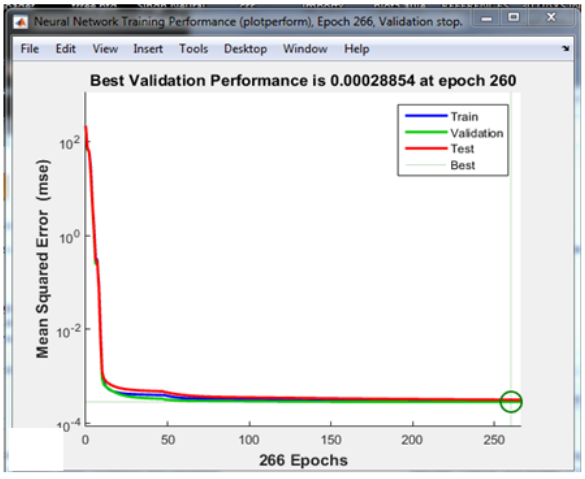


Figure 8a and b: Validation Performance Plot for Neural Network with 10 Neurons

**Table 1**: Some of the Validation Performance and other Parameters Results at different Network Architecture for Neuron 10 and 15

| Network Architecture | Best validation performance | Regression for Training | Regression for validation | Regression for Testing | Mean squared error | No. of iteration | Epoch |
|---|---|---|---|---|---|---|---|
| Net1(10) | - | 0.999996 | 0.999996 | 0.835639 | - | - | - |
| Net2(10) | 0.00034704 | 0.999996 | 0.999995 | 0.999995 | 0.000261370 | 21 | 15 |
| Net3(10) | 0.00031256 | 0.999995 | 0.999994 | 0.999914 | 0.000305995 | 72 | 58 |
| **Net4(10)** | **0.00028854** | **0.999996** | **0.999996** | **0.999996** | **0.000267208** | **64** | **260** |
| Net1(15) | 0.00033912 | 0.999996 | 0.999785 | 0.999580 | 0.000268692 | 15 | 11 |
| Net2(15) | 0.00041506 | 0.999996 | 0.999994 | 0.999995 | 0.000285503 | 17 | 9 |
| Net 3(15) | 0.00032155 | 0.999196 | 0.919995 | 0.999994 | 0.000315082 | 16 | 13 |

Figure 9 shows regression plot of the network outputs with respect to targets for training, validation, and test sets to view the plots for the best network's performance of 10 neurons. The closeness of the regression value to 1 is an indication that the fits are good while the regression value towards zero indicate a poor fit. The fit is reasonably good for all data sets, with which regression coefficient (R) values for training is 0.9996, validation is 0.99934 and test is 0.9993. The regression value on the neuron 10 for all training, validation and test simulated together is 0.9996 which is very close to 1. Since the network performance is satisfactorily good, the script was then generated.

ANN Script that has already modeled the input and output parameters of well 1 was generated in order to reproduce results (predicted porosity variables of other wells). The results (porosity) of well 2, 3, 4 and 5 were predicted using the network's script and those of wells 2 and 4 are presented in Table 2 and 3 respectively.

**Validation**

The core porosity data of well 2 and 4 available, and they were also both presented in Table 2 and 3 with their respective ANN predicted porosity for the purpose of validation. Figures 10 and 11 show the graphical plot of depth against ANN predicted porosity and core porosity of wells 2 and 4 respectively. The depth is within an interval inclusive of the target reservoir. It is evident in both graphs that the ANN predicted porosity curve mimics the core data curve.

**Statistical analyses**

Statistical analysis was also done to determine the level of correlation between the predicted porosity and actual core porosity data. Regression coefficients from the graph of predicted porosity against core porosity of well 2 and 4 are approximately equal to 1 which suggest a good correlation (Figure 12). Average percentage deviation of well 2 and 4 are 1.9031% and 11.4615%.

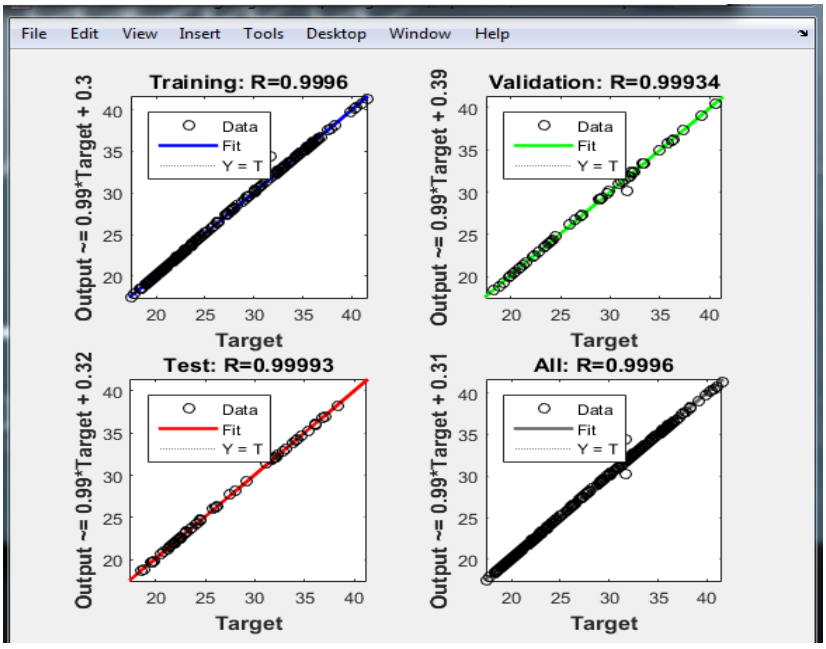


Figure 9: Regression Plot for Neural Network with 10 Neurons

**Table 2: Predicted and Core Porosities with respect to Depth of Well 2**

| Well 2 | | | | | | | | |
|---|---|---|---|---|---|---|---|---|
| Depth(ft) | Predicted Porosity (%) | Core Porosity(%) | Depth(ft) | Predicted Porosity(%) | Core Porosity(%) | Depth(ft) | Predicted Porosity(%) | Core Porosity(%) |
| 9120 | 25.06125 | 24.57143 | 9135.5 | 19.72725 | 19.37143 | 9151 | 18.71373 | 18.34286 |
| 9120.5 | 27.39931 | 26.85714 | 9136 | 19.66343 | 19.31429 | 9151.5 | 19.22282 | 18.85714 |
| 9121 | 29.13149 | 28.57143 | 9136.5 | 20.01217 | 19.65714 | 9152 | 19.5358 | 19.2 |
| 9121.5 | 30.36045 | 29.82857 | 9137 | 20.66436 | 20.28571 | 9152.5 | 19.64602 | 19.25714 |
| 9122 | 31.69106 | 31.08571 | 9137.5 | 21.24198 | 20.85714 | 9153 | 19.66915 | 19.31429 |
| 9122.5 | 33.43508 | 32.8 | 9138 | 21.45811 | 21.02857 | 9153.5 | 19.61686 | 19.25714 |
| 9123 | 34.91858 | 34.28571 | 9138.5 | 21.1602 | 20.74286 | 9154 | 19.45447 | 19.08571 |
| 9123.5 | 35.20955 | 34.57143 | 9139 | 20.58163 | 20.17143 | 9154.5 | 19.33276 | 18.97143 |
| 9124 | 34.35914 | 33.71429 | 9139.5 | 20.42629 | 20.05714 | 9155 | 19.34435 | 18.97143 |
| 9124.5 | 33.11437 | 32.51429 | 9140 | 21.58184 | 21.2 | 9155.5 | 19.39075 | 19.02857 |
| 9125 | 32.07387 | 31.48571 | 9140.5 | 24.63697 | 24.17143 | 9156 | 19.48365 | 19.14286 |
| 9125.5 | 31.82368 | 31.25714 | 9141 | 29.01353 | 28.45714 | 9156.5 | 19.84363 | 19.48571 |
| 9126 | 32.78116 | 32.17143 | 9141.5 | 32.86414 | 32.28571 | 9157 | 20.53028 | 20.17143 |
| 9126.5 | 34.40151 | 33.77143 | 9142 | 34.15234 | 33.54286 | 9157.5 | 21.25359 | 20.85714 |
| 9127 | 35.2322 | 34.57143 | 9142.5 | 32.32818 | 31.71429 | 9158 | 21.60986 | 21.2 |
| 9127.5 | 34.41518 | 33.77143 | 9143 | 28.66565 | 28.11429 | 9158.5 | 21.38186 | 20.97143 |
| 9128 | 32.55831 | 31.94286 | 9143.5 | 25.5702 | 25.08571 | 9159 | 20.57691 | 20.17143 |
| 9128.5 | 30.77918 | 30.22857 | 9144 | 24.98655 | 24.51429 | 9159.5 | 19.45544 | 19.08571 |
| 9129 | 29.88418 | 29.31429 | 9144.5 | 26.14724 | 25.65714 | 9160 | 18.52392 | 18.17143 |
| 9129.5 | 30.11073 | 29.54286 | 9145 | 26.62198 | 26.11429 | | | |
| 9130 | 30.88317 | 30.28571 | 9145.5 | 25.7911 | 25.31429 | | | |
| 9130.5 | 30.92402 | 30.34286 | 9146 | 25.02851 | 24.57143 | | | |
| 9131 | 29.8918 | 29.31429 | 9146.5 | 24.31353 | 23.82857 | | | |
| 9131.5 | 28.8257 | 28.28571 | 9147 | 22.10291 | 21.71429 | | | |
| 9132 | 28.17233 | 27.65714 | 9147.5 | 18.90079 | 18.57143 | | | |
| 9132.5 | 26.9728 | 26.45714 | 9148 | 16.96542 | 16.62857 | | | |
| 9133 | 24.60815 | 24.11429 | 9148.5 | 17.05709 | 16.74286 | | | |
| 9133.5 | 22.04647 | 21.65714 | 9149 | 17.8613 | 17.54286 | | | |
| 9134 | 20.54753 | 20.17143 | 9149.5 | 18.25872 | 17.88571 | | | |
| 9134.5 | 20.12266 | 19.71429 | 9150 | 18.27003 | 17.94286 | | | |
| 9135 | 19.96554 | 19.6 | 9150.5 | 18.33294 | 18 | | | |

**Table 3: Predicted and Core Porosities with Respect to Depth of Well 4**

| **Well 4** | | | | | | | | |
|---|---|---|---|---|---|---|---|---|
| **Depth(ft)** | **Predicted Porosity (%)** | **Core Porosity(%)** | **Depth(ft)** | **Predicted Porosity(%)** | **Core Porosity(%)** | **Depth(ft)** | **Predicted Porosity(%)** | **Core Porosity(%)** |
| 8690 | 18.67892 | 16.75452 | 8710.5 | 26.62237 | 23.85302 | 8731.5 | 38.32445 | 34.39636 |
| 8690.5 | 19.15896 | 17.17208 | 8711 | 29.22695 | 26.20178 | 8732 | 37.44642 | 33.61344 |
| 8691 | 19.43147 | 17.43306 | 8711.5 | 33.52576 | 30.06419 | 8732.5 | 36.81725 | 33.0393 |
| 8691.5 | 19.6466 | 17.64184 | 8712 | 36.92362 | 33.09149 | 8733 | 36.30085 | 32.56954 |
| 8692 | 20.7582 | 18.63354 | 8712.5 | 38.43313 | 34.44856 | 8733.5 | 35.66947 | 31.9954 |
| 8692.5 | 22.75541 | 20.40816 | 8713 | 38.81183 | 34.76172 | 8734 | 35.10126 | 31.52565 |
| 8693 | 24.18181 | 21.66083 | 8713.5 | 38.83205 | 34.81392 | 8734.5 | 35.02036 | 31.42126 |
| 8693.5 | 23.40712 | 20.9823 | 8714 | 38.62334 | 34.65733 | 8735 | 35.35006 | 31.73443 |
| 8694 | 21.67669 | 19.41646 | 8714.5 | 38.12226 | 34.18758 | 8735.5 | 36.11522 | 32.41296 |
| 8694.5 | 21.47247 | 19.25987 | 8715 | 37.79883 | 33.87441 | 8736 | 37.11952 | 33.30027 |
| 8695 | 23.69782 | 21.24328 | 8715.5 | 37.94124 | 34.031 | 8736.5 | 37.56874 | 33.71783 |
| 8695.5 | 26.79228 | 24.0096 | 8716 | 38.35863 | 34.39636 | 8737 | 36.89189 | 33.09149 |
| 8696 | 28.64874 | 25.67983 | 8716.5 | 38.92967 | 34.86611 | 8737.5 | 35.52559 | 31.83882 |
| 8696.5 | 29.0391 | 26.0452 | 8717 | 40.05194 | 35.91001 | 8738 | 34.66626 | 31.05589 |
| 8697 | 29.63213 | 26.56714 | 8717.5 | 41.20526 | 36.95391 | 8738.5 | 34.45699 | 30.89931 |
| 8697.5 | 31.53106 | 28.28957 | 8718 | 40.60761 | 36.43196 | 8739 | 34.45764 | 30.89931 |
| 8698 | 34.14431 | 30.63834 | 8718.5 | 38.4507 | 34.50075 | 8739.5 | 34.53062 | 31.0037 |
| 8698.5 | 35.7835 | 32.09979 | 8719 | 36.7564 | 33.0393 | 8740 | 34.91448 | 31.36906 |
| 8699 | 36.1965 | 32.46515 | 8720 | 38.54896 | 34.65733 | 8740.5 | 35.39705 | 31.78662 |
| 8699.5 | 36.38806 | 32.62174 | 8720.5 | 40.17144 | 36.11879 | 8740 | 34.91448 | 31.36906 |
| 8700 | 37.11889 | 33.30027 | 8721 | 41.62891 | 37.42366 | 8740.5 | 35.39705 | 31.78662 |
| 8700.5 | 37.28511 | 32.62174 | 8721.5 | 42.62227 | 38.36316 | 8741 | 35.3241 | 31.73443 |
| 8701 | 35.40257 | 33.30027 | 8722 | 42.39828 | 38.15439 | 8741.5 | 34.65922 | 31.10809 |
| 8701.5 | 31.93642 | 33.45685 | 8722.5 | 40.60871 | 36.43196 | 8742 | 34.38663 | 30.84712 |

| | | | | | | | | |
|---|---|---|---|---|---|---|---|---|
| 8702 | 29.52417 | 31.73443 | 8723 | 38.14497 | 34.23978 | 8742.5 | 35.15495 | 31.52565 |
| 8702.5 | 30.13532 | 28.65494 | 8723.5 | 36.56106 | 32.83052 | 8743 | 36.82315 | 33.09149 |
| 8703 | 32.06819 | 26.46275 | 8724 | 36.18126 | 32.46515 | 8743.5 | 38.03258 | 34.18758 |
| 8703.5 | 31.84805 | 27.0369 | 8724.5 | 36.11671 | 32.41296 | 8744 | 37.66881 | 33.82222 |
| 8704 | 28.39938 | 28.75932 | 8725 | 35.90069 | 32.20418 | 8744.5 | 35.97572 | 32.30857 |
| 8704.5 | 23.79394 | 28.55055 | 8725.5 | 36.01913 | 32.30857 | 8745 | 34.298 | 30.79492 |
| 8705 | 20.51856 | 25.41886 | 8726 | 36.61679 | 32.83052 | 8745.5 | 32.67985 | 29.33347 |
| 8705.5 | 19.50777 | 21.34767 | 8726.5 | 37.13832 | 33.35247 | 8746 | 29.99695 | 26.88031 |
| 8706 | 20.11241 | 18.42476 | 8727 | 37.48197 | 33.66563 | 8746.5 | 25.86777 | 23.17448 |
| 8706.5 | 21.54157 | 17.48525 | 8727.5 | 37.89739 | 34.031 | 8747 | 22.10184 | 19.83402 |
| 8707 | 22.99231 | 18.0072 | 8728 | 38.04039 | 34.13539 | 8747.5 | 20.21046 | 18.11159 |
| 8707.5 | 24.80587 | 19.31207 | 8728.5 | 37.74063 | 33.87441 | 8748 | 20.15752 | 18.05939 |
| 8708 | 28.26365 | 20.61694 | 8729 | 37.36449 | 33.50905 | 8748.5 | 20.69821 | 18.58134 |
| 8708.5 | 32.59469 | 22.23498 | 8729.5 | 37.53559 | 33.66563 | 8749 | 20.82661 | 18.68573 |
| 8709 | 34.44585 | 25.31447 | 8730 | 38.37551 | 34.44856 | 8749.5 | 20.40721 | 18.32037 |
| 8709.5 | 32.0202 | 29.22908 | 8730.5 | 39.08276 | 35.07489 | 8750 | 19.81435 | 17.74623 |
| 8710 | 27.9668 | 25.0535 | 8731 | 39.00021 | 34.9705 | | | |

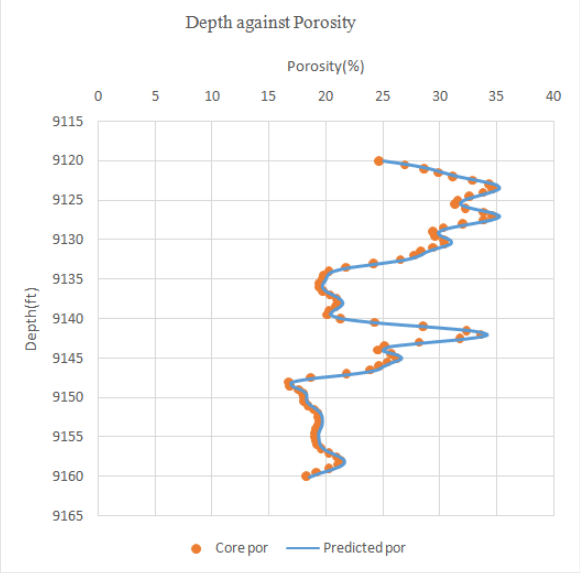


Figure 10: Correlation between Measured Core Porosity and ANN Predicted Porosity at Well 2

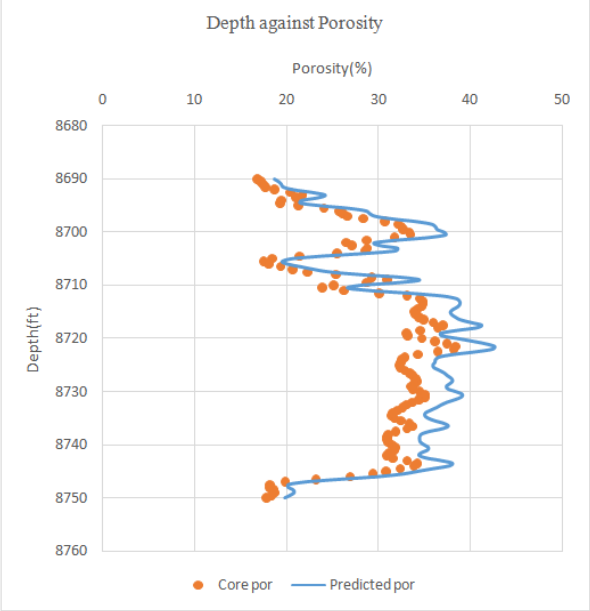


Figure 11: Correlation between Measured Core Porosity and ANN Predicted Porosity at Well 4

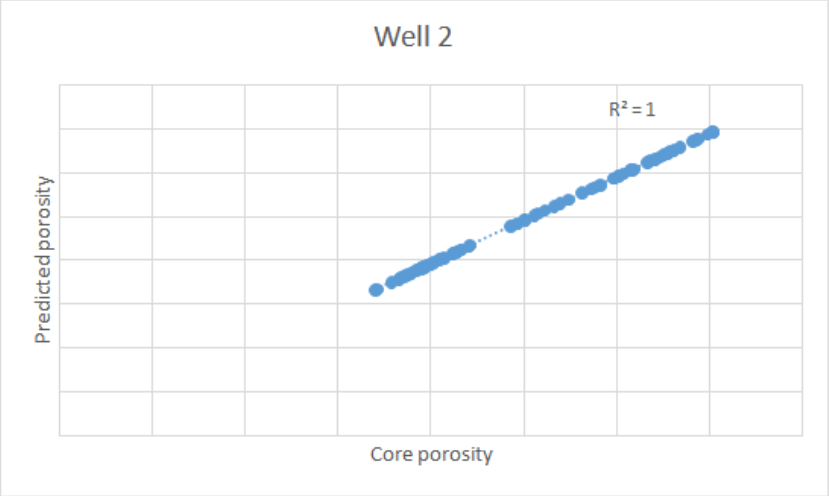


Figure 12: Cross Plot of Predicted porosity against Core Porosity for Well 2

Percentage deviation for well 2 = $\frac{0.375869381}{19.75085714} \times 100$
=1.9031%

Percentage deviation for well 4 = $\frac{4.061075184}{35.4324274} \times 100$
=11.4615%

## IV. Conclusions

Artificial neural network technique has helped the accurate prediction of reservoir porosity and understanding the real reservoir porosity condition of 'OSA' Field in Niger Delta, Nigeria. The ability of artificial neural networks to extract information from well log data, trained with core porosity data and further predict reservoir porosities has been studied to reduce high expenses of coring. The porosity predicted with the neural network approach is found more accurate than the porosity estimated through the convectional equation from the well log data. The high degree of the correlation between the core porosity and the ANN derived porosity has demonstrated the potential of the ANN method for analyzing the porous and non-porous zones of the reservoir. Neural network designed in the study can be replicated and used in other area to reliably estimate the real porosity values especially when core data is inadequate. ANN can be also employed to reveal what the conventional method is hiding in term of porosity estimation.

## References

[1]. Oyeneyin, B. (2015). Introduction to the hydrocarbon composite production system. *Elsevier, Amsterdam.* pp25.
[2]. Martin, F. David and Robert M. Colplts P. G. (1966). Reservoir Engineering. Standard Handbook of Petroleum and Natural Gas Engineering. *Gulf Publishing Company Houston, Texas.* Volume 2, pp 35.
[3]. Arabani, M. S. and Bidhendi, M. (2002). Porosity Prediction from Wireline Logs using Artificial Neural Networks: A case study in North-East of Iran. *Iranian International Journal Sci.*, pp. 3, 221-233.
[4]. Lim, J. and Kim, J. (2004). Reservoir Porosity and Permeability Estimation from Well Logs using Fuzzy Logic and Neural Network. Society of Petroleum Engineers, Spe-88476-pp. 9-12
[5]. Hyne, N. (2014). Dictionary of Petroleum Exploration, Drilling and Production (Tulsa: Penwell Corporation) pp 394-395.
[6]. Coates, G. R., Menger S., Prammer, M. and Miller, D. (1997). Applying NMR total and effective porosity to formation evaluation. In: Proceedings of the 1997 SPE Annual Technical Conference and Exhibition. Onepetro Database.
[7]. Asquith, G. and Gibson, C. (1982). Basic Well log Analysis for Geologists. *American Association of Petroleum Geologists*, pp. 15-20.
[8]. Ouenes, A. (2000). Practical application of fuzzy logic and neural networks to fractured reservoir characterization. *Computer and Geoscience* Vol. 26, pp 953-962.
[9]. Nikravesh, M. and Aminzadeh, F. (2001). Past, Present and Future Intelligent Reservoir characterization trends. *Journal Petrol. Sci. Eng.* Vol.31, pp. 67-79.
[10]. Nikravesh, M., Aminzadeh, F. and Zadeh, L. A., (2003). Soft Computing and Intelligent Data Analysis in Oil Exploration. Developments in Petroleum Sciences vol. 51. *Elsevier, Amsterdam, The Netherlands.*
[11]. Aminian, K. and Ameri, S. (2005). Application of Artificial Neural Networks for Reservoir Characterization with Limited Data. Journal Petrol. Sci. Eng., pp. 49, 212-222.

[12]. Kaydani, H., Mohebbi, A. and Baghaie, A. (2012). Neural fuzzy system development for the prediction of permeability from wireline data based on fuzzy clustering. *Petrol. Sci. Technol.*, 30, 2036-2045.
[13]. Bhatt, A. (2002).Reservoir Properties from Well Logs using neural Networks(Norway: Norwegian University of Science and Technology)
[14]. Bhatt, A. and Helle, H. B. (2002). Committee Neural Networks for Porosity and Permeability from Well Logs. *Geophysical Prospecting*. pp 56, 645-660.
[15]. Klett, T. R., Ahlbrandt, T. S., Schmoker, J. W. and Dolton, J. L. (1997). Ranking of the world's oil and gas provinces by known petroleum volumes: *U.S Geological Survey Open file Report*, pp. 97-463.
[16]. Tuttle, L. W., Brownfield, M. E. and Charpentier, R. (1999). Tertiary Niger Delta (Akata-Agbada) Petroleum System, Niger Delta province, Nigeria, pp. 66
[17]. Doust, H. and Omatsola, E.(1990).Niger Delta, in, Edwards, J. D. and Santogrossi, P.A., eds., Divergent/passive Margin Basins, AAPG Memoir 48: Tulsa, American Association of Petroleum Geologists, pp. 239-248.
[18]. Evamy, B. D., Haremboure, J., Kamerling, P., Knaap, W. A., Molloy, F. A., and Rowlands, P. H. (1978). Hydrocarbon Habitat of Tertiary Niger Delta: *American Association of Petroleum Geologists Bulletin*, vol. 62, pp. 277-298.
[19]. Shannon, P. M., and Naylor N., 1989, Petroleum Basin Studies: London, Graham and Trotman Limited, pp 153-169.
[20]. Singh, S., Kanli, A. I. and Sevgen, S. (2015). A general approach for porosity estimation using artificial neural network method: A case study from Kansas gas field. *Studia Geophysica et Geodaetica*. pp. i-ix
[21]. Dayhoff, J. E. (1990). Neural Networks Principles. Prentice-Hall International, USA. First Edition, pp. 5-36.

AKNOWLEDGEMENT
I thank Department of Petroleum Resource (DPR) with the support of Shell Nigeria Exploration and Production Company Limited for releasing the data set used for this research.
The authors whose names have been submitted certify that, they have NO affiliations with or involvement in any organization or institution or entity with any financial organization which may affect the integrity and quality of this work.
Sincerely,
**Ayantola**, Sola Oluwaseun
Corresponding Author

Sola Oluwaseun Ayantola and John Olurotimi Amigun. "Artificial Neural Network Application for Optimum Prediction of Porosity in Heterogeneous Reservoir using Well logs." *IOSR Journal of Applied Geology and Geophysics (IOSR-JAGG)*, 8(1), (2020): pp. 11-22.